Peer-reviewed version available at J. Manuf. Mater. Process. 2018, 2, 81; doi:10.3390/jmmp2040081

(Article)

Precision Permittivity Measurement for Low-Loss Thin Planar Materials Using Large Coaxial Probe from 1 to 400 MHz

Kok Yeow You[1,*] and Man Seng Sim[1]

[1]School of Electrical Engineering, Faculty of Engineering, Universiti Teknologi Malaysia, 81310, Skudai, Johor, Malaysia; kyyou@fke.utm.my

* Correspondence: kyyou@fke.utm.my; Tel.: +(6)017-9529948

Abstract: This paper focuses on the non-destructive dielectric measurement for low-loss planar materials with a thickness of less than 3 mm using a large coaxial probe with an outer diameter of 48 mm. The aperture probe calibration procedure required only to make a measurement of the half-space air and three offset shorts. The reflection coefficient for the thin material is measured using a Keysight E5071C network analyzer from 0.3 MHz to 650 MHz and then converted to a relative dielectric constant and tangent loss via closed form capacitance model and lift-off calibration process. Measurement error of dielectric constant, $\Delta\varepsilon_r$ is less than 2.5 % from 1 MHz to 400 MHz and the resolution of loss tangent, tan δ measurement is capable of achieving 3×10^{-3}.

Keywords: large coaxial probe, thin planar materials, low-loss materials, relative permittivity, reflection coefficient, calibration.

---

1. Introduction

The introduction should briefly place the study in a broad context and highlight why it is important. It should define the purpose of the work and its significance. The current state of the research field should be reviewed carefully and key publications cited. Please highlight controversial and diverging hypotheses when necessary. Finally, briefly mention the main aim of the work and highlight the principal conclusions. As far as possible, please keep the introduction comprehensible to scientists outside your particular field of research. References should be numbered in order of appearance and indicated by a numeral or numerals in square brackets, e.g., [1] or [2,3], or [4–6]. See the end of the document for further details on references. Sensitivity, sustainability and simplicity in operations are important requirements for sensing devices in large-scale material processing industries. To reduce the uncertainty of the measurements, the sensors should have large sensing area, high concentration of sensing field and high sensitivity to the slight changes in material under test (MUT). The operating frequency of the permittivity, εr measurements in most of the material processing industries are up to a few hundred MHz [1]-[3].

Open-ended coaxial probe technique is a simple, broadband and non-destructive way to measure the relative permittivity, ε_r of a material. Coaxial probes have been commercialized and used commonly since 1990 [4]. Recently, several probes have produced by manufacturers such as SPEAG Inc. [5], KEYCOM [6], and APREL Inc. [7]. However, coaxial probes (N-type's or SMA's diameter size) are less sensitive to small changes in the MUT especially for thin and low-loss materials in permittivity, ε_r measurement at MHz frequency. This causes the measurement results for low-loss materials at low frequencies to be highly scattered and less precise [8]. In fact, most

Peer-reviewed version available at J. Manuf. Mater. Process. 2018, 2, 81; doi:10.3390/jmmp2040081

coaxial probe is only suitable for half-space infinite lossy material with $\varepsilon_r' > 5$ and $\tan\delta > 0.05$ [4]-[11].

In this study, a large open-ended coaxial probe was designed to overcome those issues, which is capable of measuring the ε_r of low-loss materials having thickness of 1 mm precisely from 1 to 400 MHz. The probe design of the probe and its performance were analyzed in detail. An explicit formulation for the prediction of ε_r, which does not involve numerical inversion routines (iterative method) as in [8]-[11],[13] is used. The differences in this study compared with previous works are summarized in Table 1.

2. Large Coaxial Probe Design

2.1. Dimensions and Structure

The designed coaxial probe as shown in Figure 1 (a) is made of brass, since the material is relatively low cost and has slower surface oxidation process when it is exposed to the moisture in the air. The dimensions of the coaxial probe with outer radius of inner conductor, a = 7.5 mm and inner radius of outer conductor, b = 24.0 mm, were designed based on the characteristic impedance, $Z_o = [60\times\ln(b/a)/\sqrt{\varepsilon_c}] = 50\ \Omega$. The maximum limit of the operating frequency, fmax propagating in the coaxial line of the probe is determined using TE_{11} cut-off as: $f_{max} = (3\times10^8)/[\pi(b+a)\sqrt{\varepsilon_c}] \approx 2.1$ GHz. The symbol ε_c (Air: ε_c = 1, Teflon: ε_c = 2.06) represents the relative permittivity of material filling in the coaxial line in between the inner and outer conductor. The total weight of the coaxial probe is 2.6 kg. It has been divided into three sections: **(I)** N-type connector, which is used to connect the coaxial probe with the network analyzer via cable. **(II)** Transition section, which is a 50 mm of air-filled conical taper. The radius a and b of the conductors are increased along the transition length with a constant ratio, b/a = 2.3. Ratio, b/a = 2.3 is required to maintain Z_o = 50 Ω along the transition length to achieve low return loss and the lowest standing wave ratio (SWR) during the transformation from small to large coaxial line. **(III)** Large coaxial line section, which is a 100 mm length of 50 Ω teflon-filled coaxial line with b/a = 3.3. The Teflon isolation block is used to prevent the MUT from getting into the coaxial line. In addition, Teflon has high flexural strength, excellent chemical resistance, and high stability over a wide temperature range.

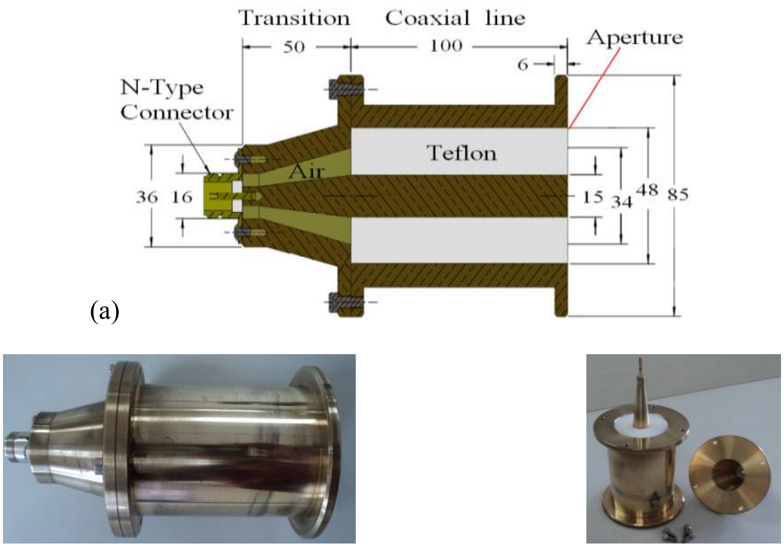

(a)

(b) (c)

Figure 1. (a) Cross-sectional side view and dimensions (in millimeter) of the coaxial sensor. (b) Side view of the large coaxial sensor. (c) Internal configuration of the coaxial sensor.

Preprints (www.preprints.org) | NOT PEER-REVIEWED | Posted: 12 October 2018 doi:10.20944/preprints201810.0263.v1

Peer-reviewed version available at J. Manuf. Mater. Process. 2018, 2, 81; doi:10.3390/jmmp2040081

Table 1. Comparative study of large probe.

Ref.	Probe size (cm)	f (MHz)	Transition section	Sample contact	Sample size/shape	Calibration standards	Measured ε_r' range	Inverse method
[8]	$2a = 1.00$ $2b = 3.25$ $L = 5.00$	100 – 900	without	Aperture probe	Half-space infinite	Air, short, NaCl solution.	~5-80	Iterative
[9]	$2a = 1.00$ $2b = 3.25$ $L = 5.00$	1 – 10 or 10–3000	without	Aperture probe	Half-space infinite	Short cavity or Air, short, short cavity	~30-80 (Lossy)	Iterative
[10]	$2a = 1.18$ $2b = 4.00$ $L \approx 13.0$	200 – 1500	with	Aperture probe	Half-space infinite	Air, copper plate, Teflon plate.	~5 - 35 (Lossy)	Iterative
[11]	$2a = 4.50$ $2b = 10.3$ $L \approx 41.0$	50 – 1000	with	Filled in coaxial line	Toroid-shaped	3 positions short-circuit along the coaxial line	~7-80 (Lossy)	Iterative
This study	$2a = 1.50$ $2b = 4.80$ $L = 15.0$	1 – 400	with	Aperture Probe	Thin planar backed by metal plate	Air, 3 offset shorts	1 - 20 (Lossless)	Non-iterative

*L is the coaxial length of the probe.

2.2. Probe Characterization Test

The complex reflection coefficient, $\Gamma_{AA'} = |\Gamma_{AA'}| \exp(j\phi_{AA'})$ at plane AA′ for four MUTs were measured using Keysight E5071C network analyzer in the frequency ranging from 0.3 MHz to 650 MHz at 25 °C. Calibration was done at the AA' plane, as shown in Figure 2, using Keysight 85032F kit.

Figure 2. Experimental set-up and measurement.

The sensing distance, h of the probe is 30 mm, which was estimated based on the distance at which the measured phase shift, $\phi_{AA'}$ (rad) as shown in Figures 3 (a) and (b) starting to become constant when the metallic plate was being moved away from the probe aperture in air. Figure 4 shows the time-domain measurements of the coaxial probe, which is operated with minimum windowing and bandpass mode. Clearly, coaxial probe of 15 cm length is sufficient to avoid the interference between plane-AA' and -BB' for the frequency-domain $\Gamma_{AA'}$ measurement.

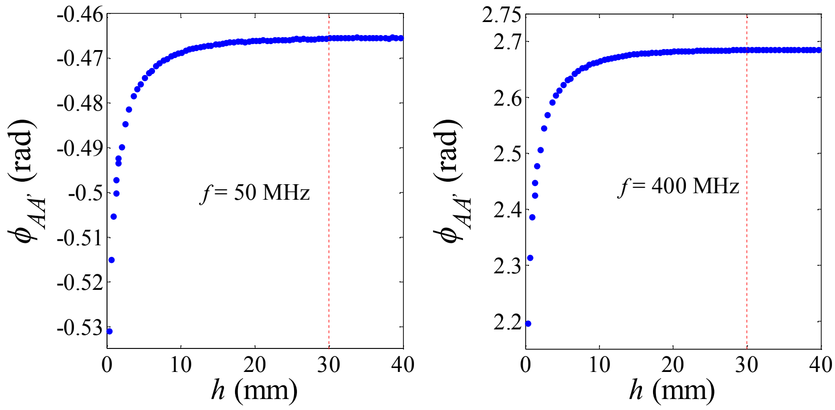

Figure 3. Variation in phase shift $\phi_{AA'}$ with air thickness, h backed by metal plate at (a) 50 MHz and (b) 400 MHz.

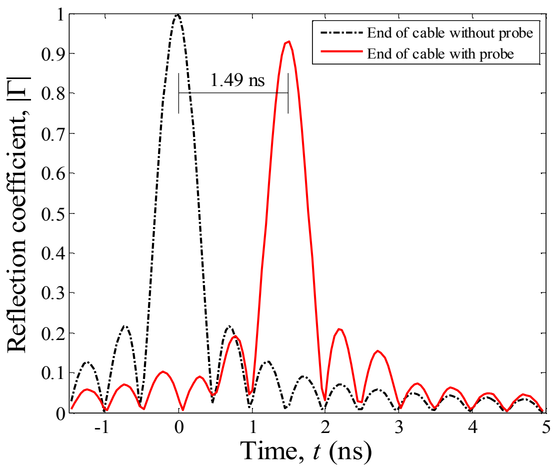

Figure 4. The time-domain response for the end of cable at plane-AA' with and without probe.

3. Calibrations

3.1. Probe Aperture Calibration

The actual normalized admittance, $\tilde{Y}_{meas}$, was measured with the aperture of the probe placed on a two-layer media, in which the first layered medium was a thin sample to be tested with thickness, h and the second layered medium was the conducting plate. The value of the $\tilde{Y}_{meas}$ of the thin sample is obtained after de-embedding using (2). The effective relative permittivity, ε_{eff} of the sample can be estimated as:

$$\varepsilon_{eff} = \left(\frac{Y_o}{j\omega C}\right)\tilde{Y}_{meas} - \frac{C_f}{C} \quad (1)$$

where

$$\tilde{Y}_{meas} = \tilde{Y}_{AA'}\left(\frac{\tilde{Y}_{BB'\_Air}}{\tilde{Y}_{AA'\_Air}}\right) \quad (2)$$

where $\tilde{Y}_{AA'\_Air}$ is the measured admittance for air at plane AA', and $\tilde{Y}_{BB'\_Air}$ is the simulated standard value of admittance for air at aperture probe (plane BB') using the COMSOL simulator. The relationship between $\Gamma_{AA'}$ and $\tilde{Y}_{AA'}$ is given as:

Preprints (www.preprints.org) | NOT PEER-REVIEWED | Posted: 12 October 2018 doi:10.20944/preprints201810.0263.v1

Peer-reviewed version available at *J. Manuf. Mater. Process.* **2018**, *2*, 81; doi:10.3390/jmmp2040081

$$\tilde{Y}_{AA'} = \frac{1-\Gamma_{AA'}}{1+\Gamma_{AA'}} \tag{3}$$

Symbol Y_o = 0.02 S, $C = 2.38\varepsilon_o(b-a)$ [11], C_f, and ω are the characteristic admittance, aperture probe capacitance, fringing field capacitance, and the angular frequency, respectively.

3.2. Effective Permittivity Calibration

For thin solid planar material measurements, the scattering of the wave from probe's aperture would penetrate the thin planar material and impinge on the other layer-interface media. In this situation, the effective permittivity, ε_{eff} of the thin specimen will be measured, but not the actual permittivity, ε_r of the material [10]. In this study, the relationship between the actual relative permittivity, ε_r and effective relative permittivity, ε_{eff} for a finite thickness planar specimen was empirically expressed as:

$$\varepsilon_r = \varepsilon_{eff}\left(a_1 + a_2 e^{-h/M} + a_3 e^{-2h/M}\right) \tag{4}$$

where h is the thickness of the specimen. The empirical coefficient, M was found to suite the large probe, which can be roughly represented by single value as 0.006 [10]. The unknown complex coefficients (a_1, a_2, and a_3) values in (4), were found by using three offset-short terminators (ε_r = 1), yield:

$$1 = \varepsilon_{eff1}\left(a_1 + a_2 e^{-h_1/M} + a_3 e^{-2h_1/M}\right) \tag{5a}$$

$$1 = \varepsilon_{eff2}\left(a_1 + a_2 e^{-h_2/M} + a_3 e^{-2h_2/M}\right) \tag{5b}$$

$$1 = \varepsilon_{eff3}\left(a_1 + a_2 e^{-h_3/M} + a_3 e^{-2h_3/M}\right) \tag{5c}$$

The unknown values of a_1, a_2, and a_3 in equations (5a)-(5c) were explicitly determined using Cramer's rule as:

$$a_1 = \frac{\left\{\begin{array}{l}\left(1/\varepsilon_{eff1}\right)\left(e^{-(h_2+2h_3)/M} - e^{-(2h_2+h_3)/M}\right) - \left(1/\varepsilon_{eff2}\right)\left(e^{-(h_1+2h_3)/M} - e^{-(h_3+2h_1)/M}\right)\\ +\left(1/\varepsilon_{eff3}\right)\left(e^{-(h_1+2h_2)/M} - e^{-(h_2+2h_1)/M}\right)\end{array}\right\}}{D} \tag{6a}$$

$$a_2 = \frac{\left\{\begin{array}{l}\left(1/\varepsilon_{eff2}\right)e^{-2h_3/M} - \left(1/\varepsilon_{eff3}\right)e^{-2h_2/M} - \left(1/\varepsilon_{eff1}\right)e^{-2h_3/M} + \left(1/\varepsilon_{eff3}\right)e^{-2h_1/M}\\ +\left(1/\varepsilon_{eff1}\right)e^{-2h_2/M} - \left(1/\varepsilon_{eff2}\right)e^{-2h_1/M}\end{array}\right\}}{D} \tag{6b}$$

$$a_3 = \frac{\left\{\begin{array}{l}\left(1/\varepsilon_{eff3}\right)e^{-h_2/M} - \left(1/\varepsilon_{eff2}\right)e^{-h_3/M} - \left(1/\varepsilon_{eff3}\right)e^{-h_1/M} + \left(1/\varepsilon_{eff1}\right)e^{-h_3/M}\\ +\left(1/\varepsilon_{eff2}\right)e^{-h_1/M} - \left(1/\varepsilon_{eff1}\right)e^{-h_2/M}\end{array}\right\}}{D} \tag{6c}$$

The determinant, D of the equations (6a)-(6c) are given as:

$$D = \left\{e^{-(h_2+2h_3)/M} - e^{-(2h_2+h_3)/M} - e^{-(h_1+2h_3)/M} + e^{-(h_3+2h_1)/M} + e^{-(h_1+2h_2)/M} - e^{-(h_2+2h_1)/M}\right\} \tag{7}$$

Preprints (www.preprints.org) | NOT PEER-REVIEWED | Posted: 12 October 2018 doi:10.20944/preprints201810.0263.v1

Peer-reviewed version available at J. Manuf. Mater. Process. 2018, 2, 81; doi:10.3390/jmmp2040081

4. Results and Discussion

Figures 5 (a) and (b) show the measured ε_r' and tan δ of four thin low-loss MUTs which are in good agreement with expected values as tabulated in Table 2. The measured scattered data in Figures 5 (a) and (b) have been smoothed by Local Polynomial Regression (Loess) algorithm, which is available in built-in MATLAB "smooth" command. The smoothed data are represented by the black solid lines in Figures 5 (a) and (b).

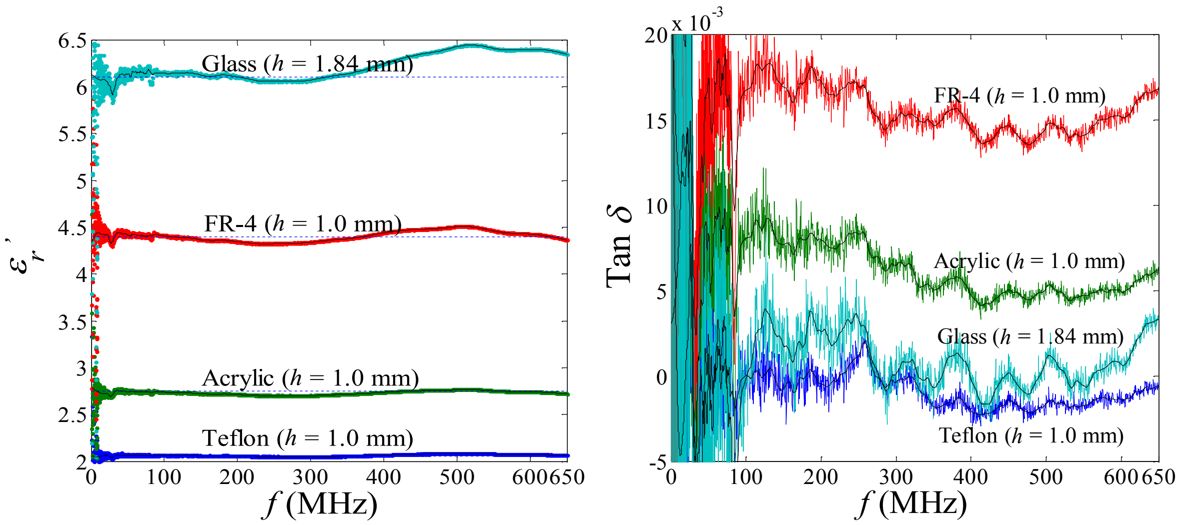

(a) (b)

Figure 5. Variation in (a) measured ε_r' and (b) measured tan δ with frequency for the MUTs at room temperature.

Table 2. Expected values for ε_r' and tan δ.

MUT	ε_r' (Typ)	tan δ (Max)
Teflon	2.06	0.0004
Acrylic	2.75	0.019
FR-4	4.4	0.022
Glass	6.1	0.0036

Figure 6 shows the percentage of the relative error between the smoothed values of ε_r' in Figure 5 (a) and the expected values of ε_r' in Table 2. The relative errors are less than 2.5 % for overall measurements from 1 MHz to 400 MHz. In addition, the resolution for measurement tan δ is capable of achieving 3×10^{-3}.

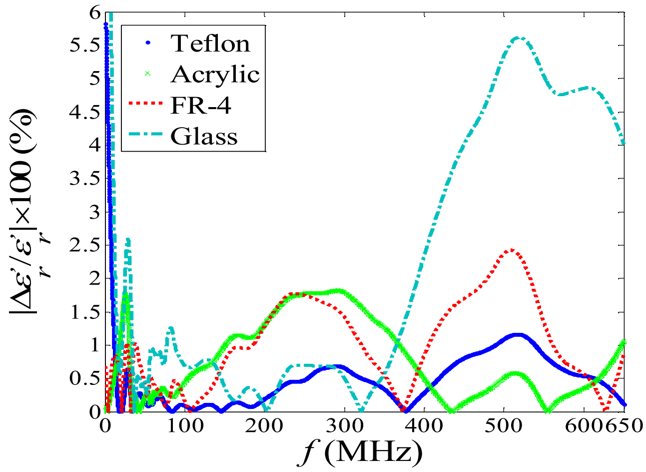

Figure 6. Variation in % relative error of ε_r'.

5. Conclusion

One-port measurement using a large coaxial probe is an easy, durable and cost effective measurement method in large-scale material processing industries. In this study, the dielectric properties for thin low-loss materials (a few millimeter thickness) at very low frequencies (below 400 MHz) have been precisely measured using the open-ended coaxial probe techniques. This accuracy level of the measurement is rarely achieved by previous studies, which used the same technique for low-loss material at very low frequencies.

Author Contributions: Conceptualization, K.Y.Y.; Methodology, K.Y.Y.; Software, K.Y.Y.; Validation, M.S.S., and K.Y.Y.; Formal Analysis, K.Y.Y. and M.S.S.; Investigation, K.Y.Y. and M.S.S.; Resources, K.Y.Y.; Data Curation, K.Y.Y.; Writing—Original Draft Preparation, K.Y.Y.; Writing—Review and Editing, K.Y.Y.; Visualization, K.Y.Y.; Supervision, K.Y.Y.; Project Administration, K.Y.Y.; Funding Acquisition, K.Y.Y.

Funding: This research was funded by i-Stone Technology and Research University Grant (GUP) from Universiti Teknologi Malaysia under project number Q.J130000.2523.15H30 and the Ministry of Higher Education of Malaysia (MOHE).

Acknowledgments: Authors would like to thank to Kok-San Chan, Shau-Lim Ooi, Tze-Lok Eng, Cha-Heng Toh for their invaluable support in probe fabrication.

Conflicts of Interest: The authors declare no conflict of interest.

References

1. Bakhshiani, M.; Suster, M. A.; & Mohseni, P. A Broadband Sensor Interface IC for Miniaturized Dielectric Spectroscopy from MHz to GHz. *IEEE Journal of Solid-State Circuits* **2014** 49(8), 1669-1681, DOI: 10.1109/CICC.2013.6658444.
2. Hegde, V. J.; Gallot-Lavallée, O.; Heux, L.. Dielectric study of Polycaprolactone: A biodegradable polymer. In, 2016 *IEEE International Conference on Dielectrics (ICD)*, 3-7 July 2016 (Vol. 1, pp. 293-296). IEEE: Montpellier, France, 2016.
3. Noh, J.; Kim, S. M.; Heo, S.; Kang, S. C.; Kim, Y.; Lee, Y. G.; ... & Lee, B. H. Time Domain Reflectometry Analysis of the Dispersion of Metal–Insulator–Metal Capacitance. *IEEE Electron Device Letters* **2017** 38(4), 521-524, DOI: 10.1109/LED.2017.2671367.
4. Hewlett-Packard. User's Manual: HP 85070B Dielectric Probe Kit. USA, 1997; Hewlett-Packard Company.
5. SPEAG. High Precision Dielectric Measurements: DAK. Switzerland, 2018; Schmid & Partner Engineering AG.
6. KEYCOM. Open Mode Probe Method Dielectric Constant and Dielectric Loss Tangent Measurement System. Japan. KEYCOM Characteristic Technologies.
7. APREL. Dielectric Probe Kit ALS-PR-DIEL. Canada, 2014; APREL Inc.

Preprints (www.preprints.org) | NOT PEER-REVIEWED | Posted: 12 October 2018 doi:10.20944/preprints201810.0263.v1

Peer-reviewed version available at *J. Manuf. Mater. Process.* **2018**, *2*, 81; doi:10.3390/jmmp2040081

8. Filali, B.; Boone, F.; Rhazi, J.; Ballivy, G. Design and Calibration of a Large Open-ended Coaxial Probe for the Measurement of the Dielectric Properties of Concrete. *IEEE Transactions on Microwave Theory and Techniques* **2008** 56(10), 2322–2328, DOI: 10.1109/TMTT.2008.2003520.
9. Otto, G. P.; Chew, W. C. Improved Calibration of a Large Open-Ended Coaxial Probe for Dielectric Measurements. *IEEE Transactions on Instrumentation and Measurement* **1991** 40(4), 742–746, DOI: 10.1109/19.85345.
10. Damme, S. V.; Franchois, A.; Zutter D. D.; Taerwe, L. Nondestructive Determination of the Steel Fiber Content in Concrete Slabs with an Open-Ended Coaxial Probe. *IEEE Transactions on Geoscience and Remote Sensing* **2004** 42(11), 2511–2521, DOI: 10.1109/TGRS.2004.837332.
11. Huang, Y. Design, Calibration and Data Interpretation for a One-port Large Coaxial Dielectric Measurement Cell. *Measurement Science Technology* **2001** 12(2001), 111–115, DOI: 10.1088/0957-0233/12/1/315.
12. Bobowski, J. S.; Clements, A. P. Permittivity and Conductivity Measured Using a Novel Toroidal Split-Ring Resonator. *IEEE Transactions on Microwave Theory and Techniques* **2017** 65(6), 2132–2138, DOI: 10.1109/TMTT.2016.2645147.
13. Shehab, F.; Myers, M. T.; Ott, H.; Dolan, S.; Dietderich, J.; Bayazitoglu, Y. Uniaxial Complex Relative Permittivity Tensor Measurement of Rocks From 40 Hz to 4.5 GHz. *IEEE Transactions on Geoscience and Remote Sensing* **2017** 55(2), 1125–1139, DOI: 10.1109/TGRS.2016.2620078.
14. Gajda, G. B.; Stuchly, S. S. Numerical Analysis of Open-Ended Coaxial Lines. *IEEE Transactions on Microwave Theory and Techniques* **1983** 31(5), 380–384, DOI: 10.1109/TMTT.1983.1131507.